Electrophoretic Motion of a Circular Cylindrical Particle in a Circular Cylindrical Microchannel

Chunzhen Ye, David Sinton, David Erickson, and Dongqing Li*

Department of Mechanical and Industrial Engineering, University of Toronto, 5 King's College Road, Toronto, Ontario, Canada, M5S 3G8

Received June 13, 2002. In Final Form: August 27, 2002

This paper investigates the electrophoretic motion of a circular cylindrical particle with hemispherical ends in a circular cylindrical microchannel filled with an aqueous electrolyte solution. The influences of three parameters on the electrophoretic motion of the particle are considered: the ratio of the particle radius to the channel radius, a/b; the ratio of the axial length of the particle to its radius, L/a; and the ratio of the zeta potential of the channel to that of the particle, $\gamma = \zeta_w/\zeta_p$. It is assumed that the electrical double layers are thin, that is, $\kappa a \rightarrow \infty$. In the analysis, the liquid phase is divided into the inner region, which consists of the electrical double layers, and the outer region, which consists of the remainder of the liquid. A theoretical model governing the inner region and the outer region has been constructed, and a force balance on the particle surface is used to determine the particle velocity. The finite element method is employed to solve the resulting set of equations. It is found that the particle velocity in a microchannel decreases as a/b increases or as L/a increases. The particle velocity is also found to decrease linearly as γ increases. On the basis of these results, an analysis of the electrophoretic separation of particles in a microchannel is presented. It is found that circular cylindrical particles of the same zeta potential, in small circular cylindrical microchannels filled with an aqueous electrolyte solution, can be separated by size.

1. Introduction

Electrophoresis is one of the most widely used separation techniques in colloidal, biological, biomedical, and biochemical science.[1−2] Electrophoretic motion of rigid particles in unbounded electrolyte solutions has been investigated extensively, and mathematical models have been developed to describe this phenomenon in detail. Summaries can be found in books by Hunter,[3] Lyklema,[4] and van de Ven.[5] However, boundary effects on the electrophoretic motion of particles need to be considered in cases where a particle moves in a channel whose size is close to the particle's size (e.g., electrophoretic motion of a protein through a porous membrane) or a particle is driven toward a solid surface. With the emergence of biochip technology, electrophoretic separation of particles in microchannels is required for lab-on-a-chip devices. Therefore, studies of the boundary effects on the electrophoretic motion of particles are important.

To date, there are some published studies on boundary effects on the electrophoretic motion of a particle. Keh et al.,[6] Ennis et al.,[7] and Shugai et al.[8] examined rigid boundary effects on electrophoretic motion of a sphere for the following cases: a sphere near a nonconducting planar wall with an electric field parallel to the wall, a sphere near a perfectly conducting planar wall with an electric field perpendicular to the wall, and a sphere on the axis of a cylindrical pore with an electric field parallel to the axis. Ennis et al.[9] experimentally investigated the electrophoretic mobility of proteins in a membrane. In addition, Zydney[10] and Lee et al.[11] investigated boundary effects on the electrophoretic motion of a charged spherical particle in a spherical cavity. However, all these results pertain to spherical particles. It is known that very few bioparticles are spherical in shape. Some protein molecules, DNA molecules, or other bioparticles are cylindrical in shape. This paper considers electrophoretic motion of a rigid circular cylindrical particle with hemispherical ends along the axis of a circular cylindrical microchannel filled with an aqueous electrolyte solution.

In this paper, the influences of three parameters on the electrophoretic motion of a circular cylindrical particle are considered: the ratio of the particle radius to the channel radius, the ratio of the axial length of the particle to its radius, and the ratio of the zeta potential of the channel to that of the particle. A developed theoretical model is described in this paper. The numerical solution to the resulting system of equations, via the finite element method, is discussed. Finally, a preliminary analysis of the electrophoretic separation of circular cylindrical particles in small circular cylindrical microchannels is presented.

2. Model

We considered a circular cylindrical particle with hemispherical ends in a circular cylindrical microchannel filled with an aqueous electrolyte solution, as shown in Figure 1a. The two ends of the microchannel are open to the atmosphere; that is, this is an open system where no

* Corresponding author. E-mail: dli@mie.utoronto.ca. Fax: (416) 978-7753.

(1) Shintani, H.; Polonsky, J. *Handbook of Capillary Electrophoresis Applications*; Blackie Academic & Professional: London, 1997.
(2) Grossman, P. D.; Colburn, J. C. *Capillary Electrophoresis*: *Theory and Practice*; Academic Press: San Diego, 1992.
(3) Hunter, R. J. *Zeta Potential in Colloid Science Principal and Applications*; Academic Press: New York, 1981.
(4) Lyklema, J. *Fundamentals of Interface and Colloid Science*; Academic Press: San Diego, 1991.
(5) van de Ven, T. G. M. *Colloidal Hydrodynamics*; Academic Press: San Diego, 1988.
(6) Keh, H. J.; Anderson, J. L. *J. Liquid Mech.* **1985**, *153*, 417−439.
(7) Ennis, J.; Anderson, J. L. *J. Colloid Interface Sci.* **1997**, *185*, 497−514.
(8) Shugai, A. A.; Carnie, S. L. *J. Colloid Interface Sci.* **1999**, *213*, 298−315.
(9) Ennis, J.; Zhang, H.; Stevens, G.; Perera, J.; Scales, P.; Carnie, S. *J. Membr. Sci.* **1996**, *119*, 47−58.
(10) Zydney, A. L. *J. Colloid Interface Sci.* **1995**, *169*, 476−485.
(11) Lee, E.; Chu, J.-W.; Hsu, J.-P. *J. Colloid Interface Sci.* **1997**, *196*, 316−320.

10.1021/la026070w CCC: $22.00
Published on Web 10/17/2002

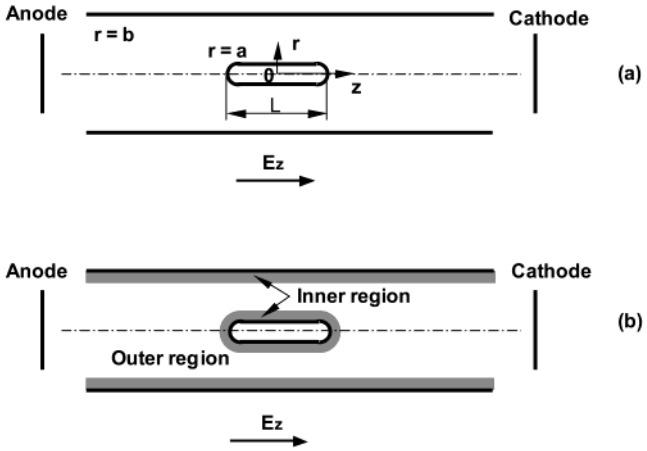

Figure 1. The schematic diagram of the particle−microchannel system: (a) the geometry of the system and (b) the division of the liquid phase.

overall pressure gradient presents in the microchannel. The particle is suspended coaxially in the microchannel. The particle has a radius a and an axial length L, and the microchannel has a radius b and an axial length l_w, where $l_w \geq 100b$. Both the particle and the channel surfaces carry uniform negative surface charges, which are characterized by their respective zeta potentials: ζ_p and ζ_w. When they are brought into contact with an electrolyte solution, there are two electrical double layers: one is surrounding the particle and the other is next to the channel wall surface. When a uniform electric field is applied along the channel, the electrophoretic motion of the particle will be toward the anode, while the electroosmotic motion of the liquid will be toward the cathode. We consider that the particle will move at a velocity U along the axis of the channel without rotation resulting from the electrophoretic motion of the particle and hydrodynamic effects of the electroosmotic flow of the liquid. To determine the particle velocity, U, a model governing the electrical field, the flow field, and the forces acting on the particle needs to be formulated and solved. Cylindrical coordinates (r, θ, z) are used with the origin located at the center of the particle; hence the particle velocity is zero, and the channel wall moves with a velocity $-U$. Due to the symmetry, all of the θ-dependent terms vanish in the subsequent analysis. To further simplify the analysis, the following four assumptions have been made: (1) Both the particle and the channel wall are rigid and nonconducting. (2) The aqueous electrolyte solution is Newtonian and incompressible; the continuity equation and the Navier−Stokes equations are valid. The flow is of low Reynolds number, so that the inertia terms in Navier−Stokes equations can be neglected. (3) The particle and the aqueous electrolyte solution are of similar density, so that the gravitational effects are negligible. (4) The electrical double layers are thin, that is, $\kappa a \rightarrow \infty$.

In this paper, we divide the liquid phase into two regions (as shown in Figure 1b): an inner region which is defined as the electrical double layers adjacent to the particle and the channel wall, where the characteristic length scale is the Debye length κ^{-1}; and an outer region which is defined as the remainder of the liquid. The following sections describe the models governing the inner and outer regions.

2.1. Inner Region. As was mentioned above, the inner region is the electrical double layer region. Variables in this region are denoted by a hat ($\wedge$) over them. At the liquid−solid interface, either on the particle or the channel wall, a local coordinate system ($\hat{y}$, $\hat{s}$) is used. The vector $\hat{y}$ is in the outward normal direction pointing into the liquid phase with $\hat{y} = 0$ at the liquid−solid interface. The scale of $\hat{y}$ is κ^{-1}, where κ^{-1} is the Debye length. The vector $\hat{s}$ is the two-dimensional position vector in the tangent plane of the solid−liquid interfaces.

In the inner region, the electrical potential, $\hat{\psi}$, is the sum of the electrical double layer potential, $\hat{\psi}_1$, and the applied electrical potential, $\hat{\psi}_2$; that is,

$$\hat{\psi} = \hat{\psi}_1 + \hat{\psi}_2 \tag{1a}$$

Since it is assumed that both the particle surface and the channel wall are nonconducting, we have the following equation at the liquid−solid interface:

$$\vec{n} \cdot \nabla\hat{\psi}_2 = 0 \tag{2}$$

where $\vec{n}$ is the unit normal vector pointing into the liquid phase. Equation 2 means that the applied electrical potential, $\hat{\psi}_2$, is dependent only on $\hat{s}$, the liquid−solid interface position vector. In the limit $\kappa a \rightarrow \infty$, it can be assumed that eq 2 prevails over the whole inner region. The potential, ψ_2, must match with the electrical potential determined from the equations of the outer region. Under the thin electrical double layer condition, Keh and Anderson[6] showed that the electrical double layer potential, $\hat{\psi}_1$, is independent of $\hat{s}$. Thus eq 1a becomes

$$\hat{\psi} = \hat{\psi}_1(\hat{y}) + \hat{\psi}_2(\hat{s}) \tag{1b}$$

where $\hat{\psi}_1$ is governed by the Poisson equation:

$$\frac{d^2\hat{\psi}_1}{d\hat{y}^2} = -\frac{\rho_e}{\epsilon\epsilon_0} \tag{3}$$

where ϵ is the dielectric constant of the electrolytic solution, ϵ_0 is the permittivity of vacuum (8.85×10^{-12} C/V m), and ρ_e is the local volume charge density.

The liquid is driven to flow in the $\hat{s}$-direction, and it is governed by the following Navier−Stokes equation:

$$\mu\frac{\partial^2\hat{v}^{(s)}}{\partial\hat{y}^2} = \rho_e\frac{\partial\hat{\psi}_2}{\partial\hat{s}} \tag{4}$$

where μ is the liquid (electrolyte) viscosity, and $\hat{v}^{(s)}$ is the tangential component of the liquid flow velocity vector $\hat{v}$. Combining eqs 3 and 4 gives

$$\mu\frac{\partial^2\hat{v}^{(s)}}{\partial\hat{y}^2} = -\epsilon\epsilon_0\frac{d^2\hat{\psi}_1}{d\hat{y}^2}\frac{\partial\hat{\psi}_2}{\partial\hat{s}} \tag{5}$$

with the following boundary conditions:

$$\frac{\partial\hat{v}^{(s)}}{\partial\hat{y}} \rightarrow 0 \quad \frac{d\hat{\psi}_1}{d\hat{y}} \rightarrow 0 \qquad \text{as } \hat{y} \rightarrow \infty \tag{6a}$$

$$\hat{v}^{(s)} = (\vec{I} - \vec{n}\vec{n}) \cdot \tilde{v} \quad \hat{\psi}_1 = \zeta \qquad \text{as } \hat{y} = 0 \tag{6b}$$

where $\vec{I}$ is the unit dyadic and $\tilde{v}$ is the velocity vector at the liquid−solid interface. $\tilde{v} = 0$ for the particle, $\tilde{v} = U\vec{e}_z$ for the channel wall, and ζ is the zeta potential at the liquid−solid interface. Integrating eq 5 twice over $\hat{y}$ with boundary conditions 6 gives

$$\hat{v}^{(s)} = \frac{\epsilon\epsilon_0}{\mu}(\zeta - \hat{\psi}_1(\hat{y}))\frac{\partial\hat{\psi}_2}{\partial\hat{s}} + (\vec{I} - \vec{n}\vec{n}) \cdot \tilde{v} \tag{7}$$

The normal component of the liquid flow velocity is

$$\hat{v}^{(y)} = \vec{n} \cdot \tilde{v} \tag{8}$$

Letting $\hat{y} \to \infty$, we can derive the tangential component of the liquid flow velocity at the outer edge of the inner region from eq 7. Combining the normal and tangential components gives the following liquid flow velocity at the outer edge of the inner region:

$$\hat{v} = \tilde{v} + \frac{\epsilon\epsilon_0\zeta}{\mu}(\vec{I} - \vec{n}\vec{n}) \cdot \nabla\hat{\psi}_2 \tag{9}$$

2.2. Outer Region. In this region, the ionic concentrations are uniform and the local volume charge density is zero. The electrical potential distribution is governed by

$$\vec{\nabla}^2\psi_2 = 0 \tag{10}$$

with the following boundary conditions:

$$\vec{n} \cdot \vec{\nabla}\psi_2 = 0 \quad \text{on the particle surface and the channel surface} \tag{11a}$$

$$\psi_2 = -E_z z \quad \text{far from the particle} \tag{11b}$$

where E_z is the applied electric strength along the channel without the suspension of the particle.

Since the local net volume charge density is zero in the bulk liquid (outer region), no body force acts on the liquid. The liquid flow in the outer region is governed by

$$\vec{\nabla} \cdot \vec{v} = 0 \tag{12a}$$

$$\mu\vec{\nabla}^2\vec{v} - \nabla\vec{p} = 0 \tag{12b}$$

where $\vec{v}$ is the liquid flow velocity vector and p is the pressure in the outer region.

The boundary conditions for eq 12 are as follows:

$$\vec{v} = \frac{\epsilon\epsilon_0\zeta_p}{\mu}(\vec{I} - \vec{n}\vec{n}) \cdot \vec{\nabla}\psi_2 \quad \text{on the particle surface} \tag{13a}$$

$$\vec{v} = U\vec{e}_z + \frac{\epsilon\epsilon_0\zeta_w}{\mu}(\vec{I} - \vec{n}\vec{n}) \cdot \vec{\nabla}\psi_2 \quad \text{on the channel surface} \tag{13b}$$

where the term "surface" in boundary conditions 11 and 13 means the outer surface of the inner region. The outer surface of the inner region encloses a neutral body (i.e., the charged particle plus the oppositely charged inner region). Therefore, the electric field produces no force on the outer surface of the inner region. At a steady state, as the particle is freely suspended in the liquid, the net force exerted by the liquid flow on the outer surface of the inner region must be zero:

$$\vec{F}_h = \int\int_S \vec{n} \cdot \vec{\sigma}\, dS = 0 \tag{14}$$

where S is the area of the outer surface of the inner region and is the stress tensor. By satisfying eq 14, one can determine the particle velocity, U.

3. Method of Calculation

From the above analysis, the liquid phase is divided into an inner region and an outer region. As κa approaches infinity, the inner region offers the boundary conditions 11a and 13 for the outer region. In the outer region, since the local net volume charge density (ρ_e) is zero, the electrical potential is contributed only by the applied electric field governed by the Laplace eq 10. The liquid flow is governed by the Stokes eqs 12, with the slipping velocity boundary conditions, eq 13. By substitution of the flow field in the force balance eq 14, the particle velocity, U, can be determined.

However, due to the nature of the system of equations and the complex geometry, it is difficult to seek an analytical solution. A numerical method is employed in this paper to obtain the solution. The first step is to nondimensionalize the governing eqs 10 and 12 and boundary conditions 11 and 13. Let

$$\vec{v}^* = \frac{\vec{v}}{U_{ep}} \tag{15a}$$

$$p^* = \frac{pa}{\mu U_{ep}} \tag{15b}$$

$$\psi_2^* = \frac{\psi_2}{\phi} \tag{15c}$$

$$r^* = \frac{r}{a} \tag{15d}$$

$$z^* = \frac{z}{a} \tag{15e}$$

$$\vec{F}_h^* = \frac{\vec{F}_h}{\mu U_{ep} a} \tag{15f}$$

where $U_{ep} = -(\epsilon\epsilon_0/\mu)\zeta_p E_z\vec{e}_z$ is used as a characteristic velocity, the particle radius, a, is set as a characteristic length scale, and $\phi = E_z a$ is a characteristic electrical potential. The stared quantities are the dimensionless variables. Substituting these variables into eqs 10 and 12 and the boundary conditions 11 and 13 yields the nondimensional equations and boundary conditions:

$$\vec{\nabla}^{*2}\psi_2^* = 0 \tag{16}$$

$$\vec{n} \cdot \vec{\nabla}^*\psi_2^* = 0 \quad \text{on the particle surface and the channel surface} \tag{17a}$$

$$\psi_2^* = -z^* \quad \text{far from the particle} \tag{17b}$$

$$\vec{\nabla}^* \cdot \vec{v}^* = 0 \tag{18a}$$

$$\vec{\nabla}^{*2}\vec{v}^* - \vec{\nabla}^* p^* = 0 \tag{18b}$$

$$\vec{v}^* = (\vec{I} - \vec{n}\vec{n}) \cdot \vec{\nabla}^*\psi_2^* \quad \text{on the particle surface} \tag{19a}$$

$$\vec{v}^* = U_p^*\vec{e}_z + \gamma(\vec{I} - \vec{n}\vec{n}) \cdot \vec{\nabla}^*\psi_2^* \quad \text{on the channel surface} \tag{19b}$$

where $U_p^* = U/U_{ep}$, which is the dimensionless particle velocity, and $\gamma = \zeta_w/\zeta_p$, which is the ratio of the zeta potential of the channel wall to that of the particle. The force balance eq 14 becomes

$$\vec{F}_h^* = \int\int_{S^*} \vec{n} \cdot \vec{\sigma}^*\, dS^* = 0 \tag{20}$$

The above nondimensionalized equations are solved through the following procedures: solve eq 16 with

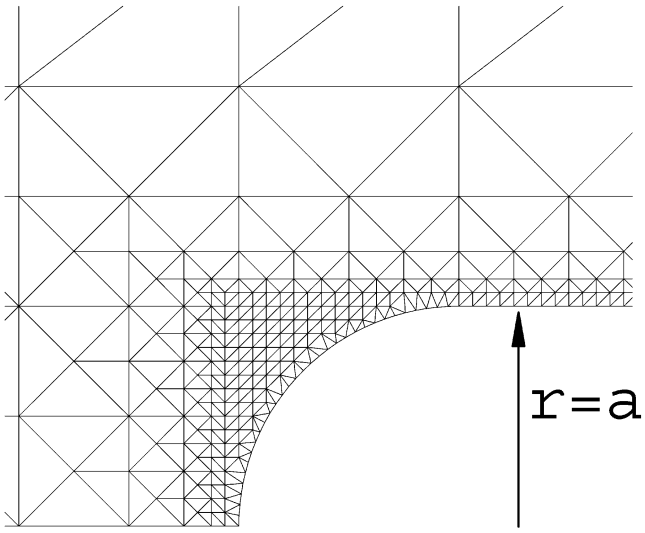

Figure 2. Illustration of fine mesh near a particle surface used in the numerical calculation.

boundary conditions 17 for the electrical potential field, substitute the calculated $\vec{\nabla}\psi_2^*$ into boundary conditions 19, solve eqs 18 with boundary conditions 19 for the flow field, and calculate the hydrodynamic force acting on the outer surface of the inner region. By satisfying eq 20, one can determine the particle velocity, U_p^*.

The finite element method[12] is employed to solve the above set of equations. An unstructured triangular mesh is used, with a fine mesh near the particle and a coarse mesh far from the particle (as shown in Figure 2). A numerical code, based on the Taylor-Hood triangle element (i.e., second-order interpolation for the electrical potential and the liquid flow velocity and first-order interpolation for the pressure), has been developed. Since the dimensionless particle velocity, U_p^*, is also involved in the boundary conditions, an iterative solution procedure is required.

To verify the code, we considered a test case: a rigid sphere with a radius a moving in a still liquid along the axis of a circular cylindrical tube with a radius b (in the absence of electrokinetic effects). For this test case, Bohlin[13] gives the formula

$$\vec{F}_z = -6\pi\mu a U_z k \vec{e}_z \tag{21}$$

$$k = \left[1 - 2.10443\frac{a}{b} + 2.08877\left(\frac{a}{b}\right)^3 - 0.94813\left(\frac{a}{b}\right)^5 - 1.372\left(\frac{a}{b}\right)^6 + 3.87\left(\frac{a}{b}\right)^8 - 4.19\left(\frac{a}{b}\right)^{10}\right]^{-1} \tag{22}$$

where $\vec{F}_z$ is the hydrodynamic force acting on the sphere when it moves at a constant velocity U_z along the axis of the tube, and k is a wall correction factor. Figure 3 compares the Bohlin formula for the wall correction factor, k, with the numerical solution of our numerical code. As can be seen, the numerical solution matches Bohlin's formula very well.

Furthermore, the electrophoretic motion of a rigid sphere with a radius a along the axis of a circular cylindrical pore of a radius b was used to test the above

(12) Johnson, C. *Numerical solution of partial differential equations by the finite element method*; Cambridge University Press: New York, 1987.

(13) Happel, J. *Low Reynolds number hydrodynamics*, 2nd ed.; Noordhoff International Publishing: Leyden, 1973; Chapter 7.

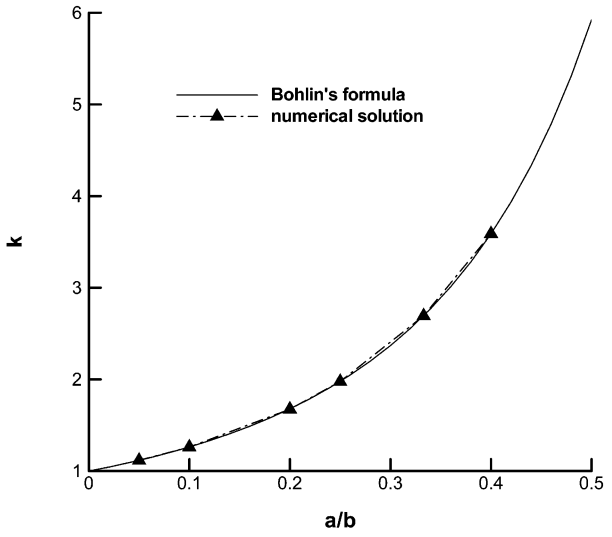

Figure 3. Comparison between Bohlin's formula and the model in this work of the wall correction factor, k, versus the ratio of a particle radius to a tube radius, a/b, for a rigid sphere moving in a stationary liquid along the axis of a circular cylindrical tube.

model and the numerical code. In the limit of a thin electrical double layer, Keh et al.[6] derived the following approximate solution by a method of reflections:

$$U = \left[1 - 1.28987\left(\frac{a}{b}\right)^3 + 1.89632\left(\frac{a}{b}\right)^5 - 1.02780\left(\frac{a}{b}\right)^6 + O\left(\left(\frac{a}{b}\right)^8\right)\right]\frac{\epsilon\epsilon_0}{\mu}(\zeta_p - \zeta_w)E_z\vec{e}_z \tag{23}$$

where U is the sphere velocity. From the above equation, the following dimensionless sphere velocity can be derived:

$$U_p^* = \frac{U}{U_{ep}} = \left[1 - 1.28987\left(\frac{a}{b}\right)^3 + 1.89632\left(\frac{a}{b}\right)^5 - 1.02780\left(\frac{a}{b}\right)^6 + O\left(\left(\frac{a}{b}\right)^8\right)\right](1 - \gamma) \tag{24}$$

Figure 4 compares Keh's solution with our numerical solution at $\gamma = 0.6$. As can be seen, the numerical solution matches Keh's solution very well.

4. Results and Discussion

As mentioned before, the purpose of this study is to investigate the influences of three parameters on the electrophoretic motion of a circular cylindrical particle in a circular cylindrical microchannel: the ratio of the particle radius to the channel radius, a/b; the ratio of the axial length of the particle to its radius, L/a; and the ratio of the zeta potential of the channel to that of the particle, $\gamma = \zeta_w/\zeta_p$. Figure 5 shows the streamlines of the flow field near the particle and the contours of the absolute value of the flow velocity at $a/b = 1/4$ and $\gamma = 0.6$. In this figure, the darker areas at the ends of the particle denote the lower flow velocity regions and the lighter areas on the sides of the particle denote the higher velocity regions.

4.1. Influence of the Ratio of Particle Radius to Channel Radius (a/b). Figure 6 shows the dimensionless particle velocity, U_p^*, versus a/b, with $\gamma = 0.6$. As can be seen, U_p^* decreases with a/b. The effect becomes stronger when the ratio of the particle's axial length to its radius increases. Compared with a spherical particle, the influence of a/b on U_p^* for a circular cylindrical particle is

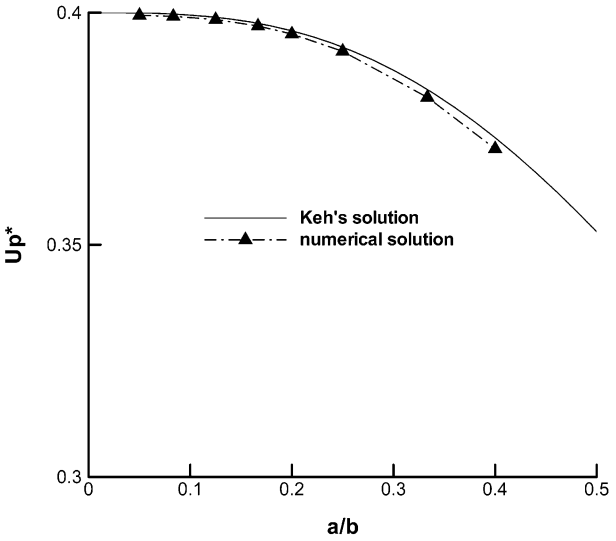

Figure 4. Comparison between Keh's solution and the model in this work of the dimensionless particle velocity, U_p^*, versus the ratio of a particle radius to a channel radius, a/b, with $\gamma = 0.6$ for the electrophoretic motion of a rigid sphere along the axis of a circular cylindrical pore.

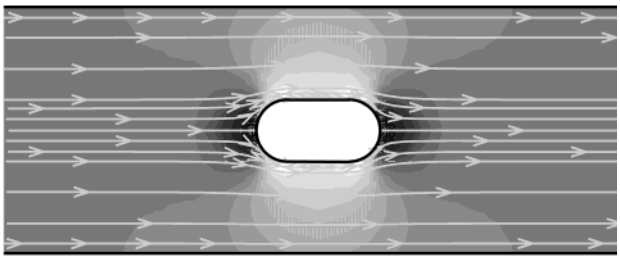

Figure 5. Streamline plot of the flow field near the particle with a contour plot of absolute values of flow velocity at $a/b = 1/4$, $L/a = 4$, and $\gamma = 0.6$.

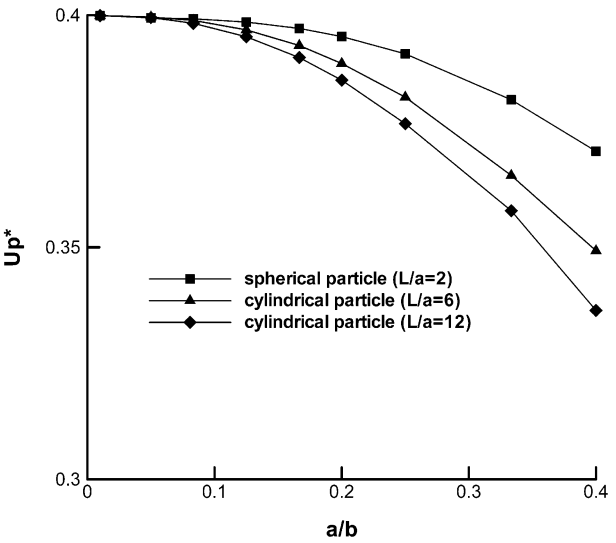

Figure 6. Calculated dimensionless particle velocity, U_p^*, versus the ratio of a particle radius to a channel radius, a/b, with $\gamma = 0.6$.

stronger. When the channel radius is far larger than the particle radius, that is, $a/b < 1/20$, the boundary effect is negligible. However, for the cases of $a/b \geq 1/20$, the boundary effect is relatively significant. This result implies that for a given channel size, the cylindrical particles with a smaller radius move faster, where the particles are assumed to have the same zeta potential and the same

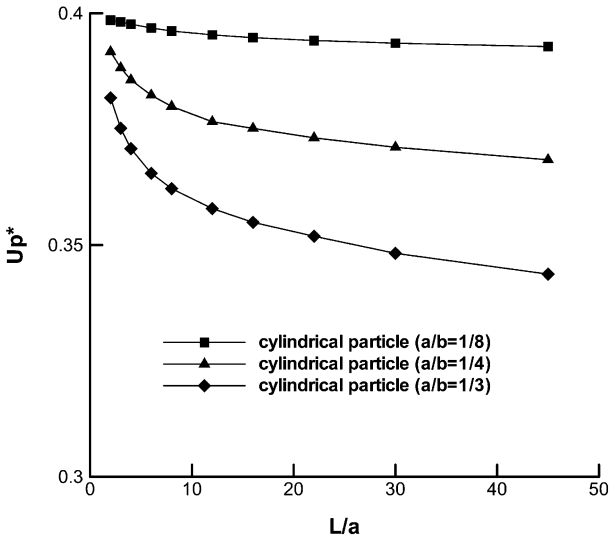

Figure 7. Calculated dimensionless particle velocity, U_p^*, versus the ratio of a particle axial length to its radius, L/a, with $\gamma = 0.6$.

Table 1. Time Required for a Cylindrical Particle Moving through a 50 mm Long Circular Cylindrical Microchannel with $a = 1$ μm, $\epsilon = 80.1$, $\zeta_w = -48$ mV, $\zeta_p = -80$ mV, $E_z = 300$ V/cm, and $\mu = 1.003 \times 10^{-3}$ kg/(m s)

	a/b								
	1/3			1/4			1/8		
L (μm)	4	6	8	4	6	8	4	6	8
U_p^*	0.371	0.365	0.362	0.386	0.382	0.380	0.398	0.397	0.396
U (mm/s)	0.628	0.619	0.614	0.654	0.648	0.644	0.674	0.673	0.671
t (s)	79.56	80.72	81.46	76.50	77.16	77.65	74.19	74.34	74.46

axial length but different radii. In other words, particles of the same zeta potential and length can be electrophoretically separated by their radii in an aqueous solution in a microchannel. A separation analysis is presented in section 4.4.

4.2. Influence of the Ratio of the Particle's Axial Length to its Radius (L/a). Figure 7 shows the dimensionless particle velocity, U_p^*, versus L/a, with $\gamma = 0.6$. As can be seen, the influence of L/a on U_p^* becomes stronger as a/b increases. For a given a/b, U_p^* decreases with L/a and gradually approaches a constant. The slope of the U_p^* versus L/a curves is steeper in the range of $L/a < 10$; that is, the particle's motion is more sensitive to L/a in this range. As shown in Table 1, to move through a 50 mm long cylindrical microchannel, when particle radii are set the same, the particle with a shorter axial length moves faster and spends less time. That is, circular cylindrical particles of the same zeta potential and the same radius can be electrophoretically separated by their axial lengths in an aqueous solution in a microchannel. A separation analysis is presented in section 4.4.

4.3. Influence of the Zeta Potential Ratio ($\gamma = \zeta_w/\zeta_p$). Figure 8 shows the dimensionless particle velocity, U_p^*, versus γ, with $a/b = 1/5$ and $L/a = 6$. U_p^* is shown to decrease linearly with γ. It is known that the electrophoretic velocity of a particle is proportional to its zeta potential, ζ_p, and that the electroosmotic flow velocity is proportional to the zeta potential of the boundary surface, ζ_w. In this system, the particle velocity is a result of the electrophoretic motion of the particle and the hydrodynamic effects of the surrounding electroosmotic flow of the liquid in the microchannel. As we consider that the particle and the channel wall carry the same type of charge

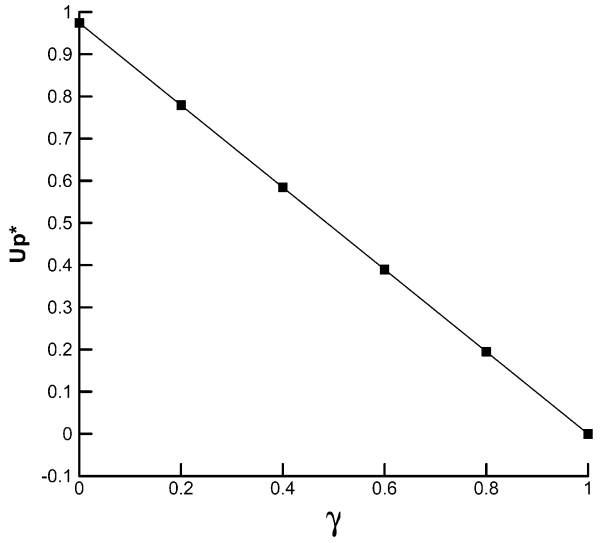

Figure 8. Calculated dimensionless particle velocity, U_p^*, versus the ratio of the zeta potential of the channel to that of the particle, γ, with $a/b = 1/5$ and $L/a = 6$.

(i.e., both positive or both negative), the electrophoretic motion of the particle is in the opposite direction to the electroosmostic flow of the liquid. In the limit of $\kappa a \rightarrow \infty$, the particle velocity is proportional to $(\zeta_p - \zeta_w)$. As shown in Figure 8, particle velocity is zero when the zeta potentials are equal (i.e., $\gamma = 1$).

4.4. Electrophoretic Separation of Circular Cylindrical Particles in a Microchannel. Electrophoresis is one of the most widely used separation techniques. It is known that the electrophoretic mobility of a particle is proportional to its zeta potential.[3] Therefore, particles with the same size but different zeta potentials can be electrophoretically separated. In the limit of a thin electrical double layer, the electrophoretic motion of a particle (U_0) in an unbounded aqueous electrolyte solution can be expressed by Smoluchowski's formula,[3] $U_0 = (\epsilon\epsilon_0\zeta_p/\mu)E_\infty$, where E_∞ is an applied electric strength. It implies that the particle's velocity is independent of its size or shape so that particles with the same zeta potential cannot be separated electrophoretically by their size or shape in unbounded aqueous solutions. However, for spherical particles moving in small channels, it is found that the particle's velocity is dependent on its size (Figure 4) and hence the spherical particles with the same zeta potential can be separated by size in microchannels. This is possible even in an unbounded liquid, if the double layer is not thin or if ka is finite as the mobility depends on ka. As for circular cylindrical particles in small circular cylindrical microchannels, our model analysis and numerical results indicate that the particle's velocity is dependent on its size, due to the boundary (channel wall) effects.

An analysis of electrophoretic separation of circular cylindrical particles in a circular cylindrical microchannel filled with an aqueous electrolyte solution is presented below. In the calculations, the following conditions were used: $\epsilon = 80.1$, $\zeta_w = -48$ mV, $\zeta_p = -80$ mV, $E_z = 300$ V/cm, and $\mu = 1.003 \times 10^{-3}$ kg/(m s). First, we considered three circular cylindrical particles with different radii, 0.5, 1, and 1.5 μm, and with the same axial length, $L = 6$ μm, in a circular cylindrical microchannel of radius $b = 12$ μm. The numerical analysis shows that these three particles have velocities of 0.677, 0.676, and 0.674 mm/s, respectively. As shown in Figure 9, the three particles are well separated after 500 s; the particle of the smallest radius moves the fastest. Here we assumed that each particle

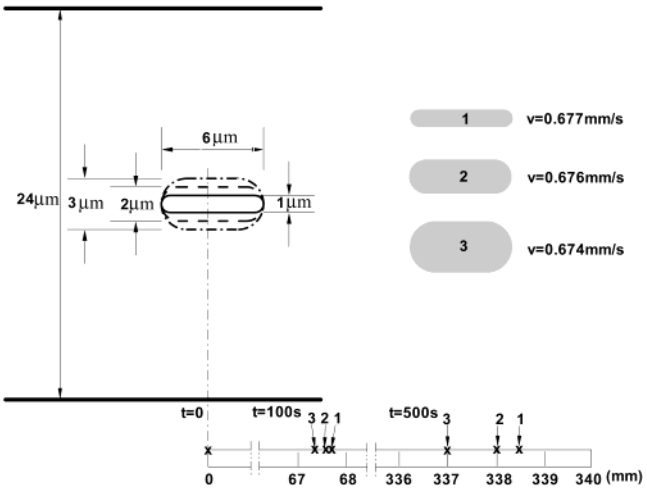

Figure 9. Illustration of circular cylindrical particles separated by their radii in a circular cylindrical microchannel with $L = 6$ μm, $b = 12$ μm, $\epsilon = 80.1$, $\zeta_w = -48$ mV, $\zeta_p = -80$ mV, $E_z = 300$ V/cm, and $\mu = 1.003 \times 10^{-3}$ kg/(m s).

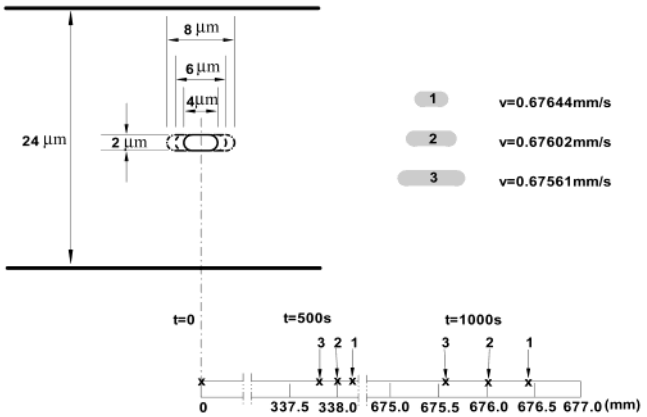

Figure 10. Illustration of circular cylindrical particles separated by their axial lengths in a circular cylindrical microchannel with $a = 0.5$ μm, $b = 10$ μm, $\epsilon = 80.1$, $\zeta_w = -48$ mV, $\zeta_p = -80$ mV, $E_z = 300$ V/cm, and $\mu = 1.003 \times 10^{-3}$ kg/(m s).

moves at a velocity as it moves along the axis of the channel in the absence of other particles. In Figure 10, another three particles with the same radius, $a = 1.0$ μm, but different axial lengths, 4, 6, and 8 μm, in a circular cylindrical microchannel of radius $b = 12$ μm were considered. Under the same conditions, these particles move at 0.67644, 0.67602, and 0.67561 mm/s, respectively. As shown, these particles can be well separated after 1000 s; the shortest particle moves the fastest.

5. Conclusion

This paper considered the electrophoretic motion of a circular cylindrical particle with hemispherical ends in a circular cylindrical microchannel filled with an aqueous electrolyte solution. The purpose is to investigate the boundary effects on the electrophoretic motion of the particle. The liquid phase is divided into the inner region and the outer region. Thin electrical double layers are assumed. In the inner region, the liquid is driven to flow by the electric field in the tangential plane. The boundary conditions for the outer region can be derived analytically from the inner region. In the outer region, the electric field is subject to the Laplace equation and the flow field is governed by the Stokes equations with slipping boundary conditions. By satisfying the force balance on the particle surface, one determines the particle velocity in

the microchannel. The finite element method was employed to solve the system of equations.

As predicted by the numerical simulations, in a circular cylindrical microchannel, the boundary effects on the electrophoretic motion of a circular cylindrical particle are appreciable when the ratio of the particle radius to the channel radius, a/b, is large and when the ratio of the axial length of the particle to its radius, L/a, is small. The dimensionless particle velocity, U_p^*, decreases with a/b for a fixed L/a, and U_p^* decreases with L/a for a fixed a/b. It was found also that U_p^* decreases as the ratio of the zeta potential of the channel to that of the particle increases. On the basis of these results, in a small circular cylindrical microchannel filled with an aqueous electrolyte solution, circular cylindrical particles of the same zeta potential may be separated electrophoretically by their radii or by their axial lengths.

The numerical calculation method presented in this work is suitable to the two-dimensional steady-state particle−liquid system. However, it is not advisable to expand this technique to more complicated cases such as three-dimensional unsteady-state particle−liquid systems. In this method, hydrodynamic force needs to be calculated explicitly. How to calculate this force accurately is a big challenge. Furthermore, if the rotational effects of the particle cannot be neglected in some more complicated cases, the interacting moments between the particle and the surrounding liquid need to be determined explicitly too. In addition, extra governing equations of rotational equilibrium/dynamics will complicate the iterative solving procedures. For these more complicated situations, direct numerical formulation[14] should be used. Furthermore, in this numerical simulation, the ratio of the particle's radius to the channel's radius, a/b, was chosen to be less than 0.5. There are two basic reasons: First, if the ratio a/b is close to unity, the gap between the particle and the channel wall is very small and the continuum and Stokes equations might not be valid in some cases. Second, for large a/b values, or the very small gaps between the particle and the channel wall, the flow velocity changes more abruptly in this gap and a finer mesh system is required to describe the flow field. This would cause more complication in the numerical calculation and decrease the accuracy.

Acknowledgment. This research was supported by a Connaught Scholarship from the University of Toronto to C. Ye and by the Natural Science and Engineering Research Council (NSERC), through postgraduate scholarships to D. Sinton and D. Erickson and a research grant to D. Li.

LA026070W

(14) Hu, H. *Int. J. Multiphase Flow* **1996**, *22*, 335−352.